SANDIA REPORT

SAND2014-18131
Unlimited Release
Printed September, 2014

Ion Channeling Revisited

Barney L. Doyle, Aldo Corona, Anh Q. Nguyen

Prepared by
Sandia National Laboratories
Albuquerque, New Mexico 87185 and Livermore, California 94550

Sandia National Laboratories is a multi-program laboratory managed and operated by Sandia Corporation, a wholly owned subsidiary of Lockheed Martin Corporation, for the U.S. Department of Energy's National Nuclear Security Administration under contract DE-AC04-94AL85000.

Issued by Sandia National Laboratories, operated for the United States Department of Energy by Sandia Corporation.

Available to DOE and DOE contractors from
U.S. Department of Energy
Office of Scientific and Technical Information
P.O. Box 62
Oak Ridge, TN 37831

Telephone: (865) 576-8401
Facsimile: (865) 576-5728
E-Mail: reports@adonis.osti.gov
Online ordering: http://www.osti.gov/bridge

Available to the public from
U.S. Department of Commerce
National Technical Information Service
5285 Port Royal Rd.
Springfield, VA 22161

Telephone: (800) 553-6847
Facsimile: (703) 605-6900
E-Mail: orders@ntis.fedworld.gov
Online order: http://www.ntis.gov/help/ordermethods.asp?loc=7-4-0#online

SAND2014-18131
Unlimited Release
Printed September 2014

Ion Channeling Revisited

Barney L. Doyle, Aldo Corona, Anh Q. Nguyen
Radiation Solid Interactions Department 01111
Sandia National Laboratories
P.O. Box 5800
Albuquerque, New Mexico 87185-MS1056

Abstract

A MS Excel program has been written that calculates accidental, or unintentional, ion channeling in cubic bcc, fcc and diamond lattice crystals or polycrystalline materials. This becomes an important issue when simulating the creation by energetic neutrons of point displacement damage and extended defects using beams of ions. All of the tables and graphs in the three Ion Beam Analysis Handbooks that previously had to be manually looked up and read from were programed into Excel in handy lookup tables, or parameterized, for the case of the graphs, using rather simple exponential functions with different powers of the argument. The program then offers an extremely convenient way to calculate axial and planar half-angles and minimum yield or dechanneling probabilities, effects on half-angles of amorphous overlayers, accidental channeling probabilities for randomly oriented crystals or crystallites, and finally a way to automatically generate stereographic projections of axial and planar channeling half-angles. The program can generate these projections and calculate these probabilities for <uvw> axes and [hkl] planes up to (555).

(Page intentionally left blank)

CONTENTS

FIGURES

(Page intentionally left blank)

1. INTRODUCTION

The three Ion Beam Analysis (IBA) Handbooks [1,2,3] have been an extremely useful references to practitioners of these techniques. However, because they first came out when powerful desk top computers were not that common, many of the calculations still must involve the manual interpolation from tables and readings from graphs. This was particularly true for the chapters on Ion Channeling written by Appleton and Foti [4], Swanson [5], and Swanson and Shao [6].

This paper strives to ameliorate this situation, at least for ion channeling, by presenting the background for a program that has been developed at Sandia National Laboratories that has been programed in universally available MS Excel, together with macros in Visual Basic Applications (VBA), making it facile to calculate channeling half angles $\psi_{1/2}$ and minimum yields, i.e. dechanneling probabilities, $\chi_{\min}$. This report is intended to document the parameterizations and lookup tables that have been made, and accompany the program as a guide.

There has been a resurgence of interest in ion channeling. From the standpoint of ion beam analysis (IBA) this includes the use of backscattering of finely focused and scanned low energy He ions from a He-Ion Microscope (HIM) [7] to observe the crystalline texture of poly/nano crystalline materials, much like is done with the analysis of Kikuchi patterns used by the electron backscatter diffraction (EBSD) technique. Ion channeling is also becoming of interest to materials scientists as regards the effect of unintentional channeling of ions used to simulate neutron induced displacement damage in polycrystalline materials [8], and intentional channeling to improve the sidewall roughness of ion-sputtered craters [9]. If the ions accidentally channel in individual crystallites in polycrystalline materials, less displacement damage will result as compared to the case where they do not channel. It is therefore important to know and quantify how this grain-by-grain disparate generation of damage can affect mechanical properties.

2. APPROACH

This paper is mainly focused on the calculation and graphical representation of accidental channeling described above, but is applicable as well for the IBA and sputtering cases. We present a solution to the problem of quickly calculating unintentional channeling probability by describing an approach that involves reproducing all the tables in the channeling chapters of the three IBA handbooks into convenient tables in MS Excel where the Lookup command can be used to retrieve the necessary beam and material target parameters. In addition to the tables, all four of the theoretical calculations presented graphically in these handbooks have been

parameterized with simple exponential functions where the argument of the exponential is taken to various powers, in order to fit the calculations presented in the graphs.

From the automated input from the tables, and direct determination of the values of the complicated Monte-Carlo determined functions displayed previously only in graphical form, the channeling half-angles $\psi_{1/2}$ and dechanneling probabilities $\chi_{\min}$ for both axial and planar channeling are easily and conveniently determined by the program. From these calculations, the probability of unintentional or accidental channeling can be determined.

Stereographic projections of the axial and planar channeling have long been used, and are central to the information provided in the IBA Handbooks, to enable practitioners of channeling a graphical way of rotating samples with multi-axes goniometers to align beams with axes and planes. But the projections in the IBA handbooks are only for low index axial <uvw> and planar [hkl] crystalline orientations, and there is no indication in the plots of the magnitude of $\psi_{1/2}$ for axes and planes. This type of visualization is extremely import in the case of accidental channeling, and of the quantitative determination of crystallite orientation using the HIM scanned channeling technique discussed above. With this computationally automated approach to the calculation of $\psi_{1/2}$ half angles, these projections are easily extended almost indefinitely, i,e $(\infty\infty\infty)$. However, one must take care in over interpreting these results for the extremely high order axial and planar channeling calculations of $\psi_{1/2}$ of axes or planes, as that is probably beyond the original channeling theorist's intent or guidance. For this reason we limit ourselves here to calculations of $\psi_{1/2}$ for axes and planes to (555).

In the following two sections we discuss 1) the determination of values used in the channeling calculations obtained from the IBA Handbook Tables, 2) the parameterization of the theoretical values in graphs, 3) the generation of stereographic projections useful in visualizing both accidental and intentional channeling experiments.

3. THE CHANNELING EQUATIONS AND THEIR CALCULATION

We will not be re-deriving the channeling theories developed by Lindhard nearly 50 years ago, nor the supplements to his theory over the years, as all of this information is readily available in any of the IBA Handbooks. We will, however reproduce the equations that appear in Swanson's Appendix 15 [5] in the second Handbook [2], as this provides the most convenient collection of all the equations used in channeling half-angles $\psi_{1/2}$ and dechanneling probabilities $\chi_{\min}$. We will refer to the MS Excel program simply as the program from now on.

3.1 Axial Channeling

3.1.1 Axial $\psi_{1/2}$ half-angles

The specular or characteristic axial channeling angle ψ_1 is calculated using the formula given in Lindhard's famous paper [10]:

$$\psi_1 = \sqrt{\frac{2Z_1 Z_2 e^2}{Ed}} \ (radians) \ , \tag{3.1}$$

Where Z_1 and E are the atomic number and Energy (MeV) of the projectile, Z_2 is the atomic number of the target atom, e is the fundamental electron charge which equals 1.44×10^{-5} MeV-*Å* and *d* is the separation of the atoms in *A* along the axial direction <uvw>.

Values for factors, f_a , the conventional cell lattice constant needs to be multiplied to calculate *d,* are given in Table A15.1 in [5] for bcc, fcc and diamond lattices, but only up to <111> axes. The determination of *d* is actually fairly complicated. After entering Z_2 in the program, a lookup table is used to find the conventional cell lattice constant, cc, in *Å* and the symmetry of the crystal lattice, i.e. bcc, hcp or diamond. For now only cubic lattices are considered. When a <uvw> axial direction is entered, the program calculates the vectors to all the atoms with vector lengths less than that of <uvw> and checks for alignment with <uvw>. It then calculates d using the axial lattice constant factor:

$$f_a = \frac{\sqrt{u^2 + v^2 + w^2}}{1 + N} \ , \tag{3.2}$$

where *N* is the number of atoms between and along the same direction as <uvw>. In general, *N=0* except *N=1* when uvw are all odd with no zeros for bcc, uvw have two indexes odd and one even including zero for fcc, and uvw are all odd or have two indexes odd and one even including zero. As a simple example, for bcc, *N*=1 for the <111> axis. *d* for each <uvw> axes is calculated by multiplying the corresponding f_a factor by the conventional cell lattice constant.

The quantity u_1 represents the vibrational amplitude of the atoms perpendicular to the axis and is expressed as:

$$u_1 = 12.1 \left(\left(\frac{\phi_D(x'')}{x''} + 0.25 \right) \left(\frac{1}{M_2 \theta_D} \right) \right)^{1/2} \ (Å), \tag{3.3}$$

Where θ_D is the Debye temperature, M_2 is the target atom mass in amu. Both of these values are also obtained after Z_2 is entered in the program using a lookup table, and

$$x'' = \frac{\theta_D}{T} \ . \tag{3.4}$$

$\phi_D(x'')$ is the Debye function, which has been parameterized here to be:

$$\phi_D(x'') = \exp(-x''/4.3) \tag{3.5}$$

The fit to the Debye function plotted in A15.1 in [5] using this equation is shown in Fig. 1.

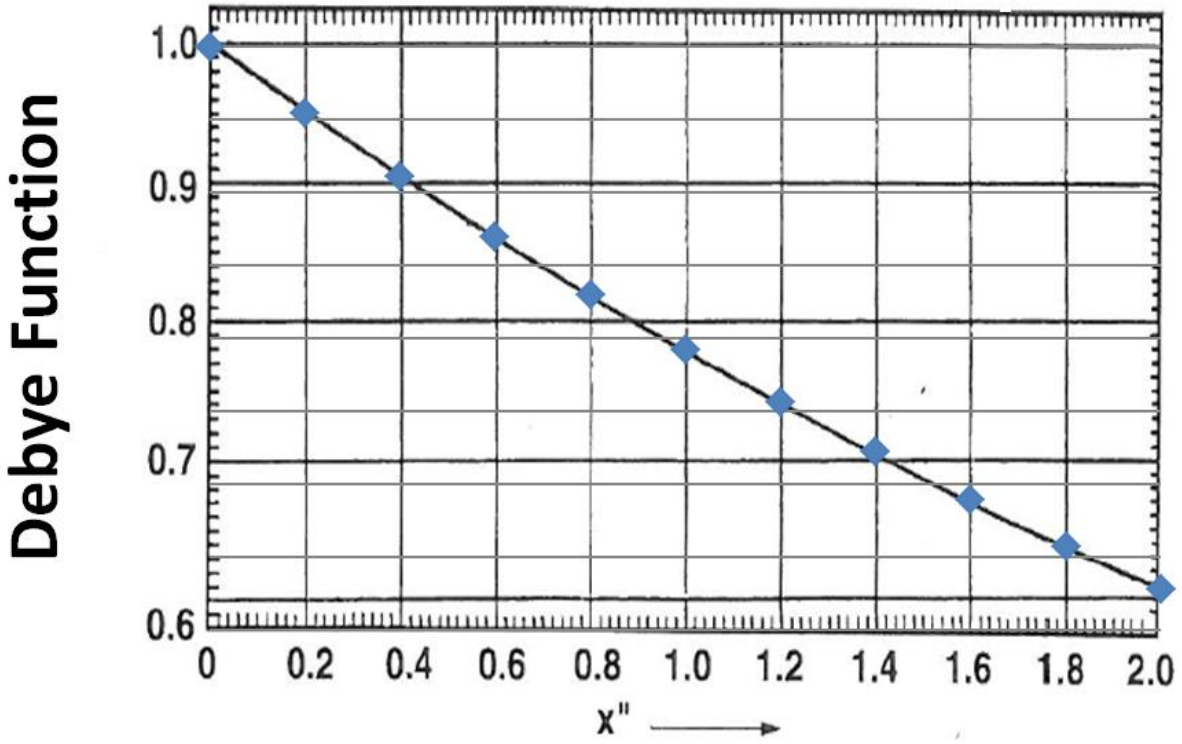

Figure 1 Parameterized Debye Function

A parameter x' relates the vibration amplitude to the Thomas-Fermi screening length, a in the equation:

$$x' = 1.2\frac{u_1}{a} \tag{3.6}$$

Several different expressions for *a* can be found in the Handbooks, but as will be discussed later, the one that provided the best agreement with the channeling data listed in the Handbooks was that of Firsov [11]:

$$a = 0.04685 / (Z_1^{2/3} + Z_2^{2/3})^{1/2} \tag{3.7}$$

The expression for the axial $\psi_{1/2}$ half angles given in [5] is:

$$\psi_{1/2} = 0.8 F_{RS}(x')\psi_1 \text{ for } \psi_1(rad) < \frac{a}{d} \tag{3.8}$$

Where F_{RS} is the square root of the adimensional string potential using Moliere's screening function and calculated using Monte Carlo techniques by Barrett [12]. The parameterized fit to the F_{RS} function plotted in A15.2 in [5] is shown in Fig. 2.

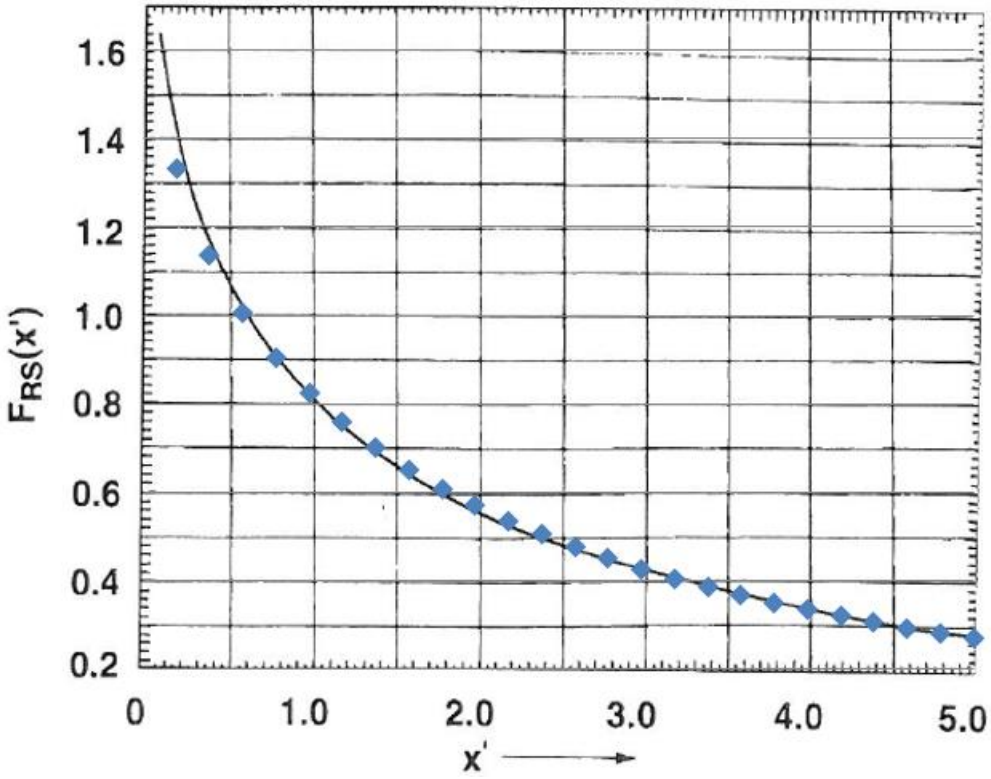

Figure 2 Parameterization of the F_{RS} adimensional function for axial channeling

The functional form of this parameterization was found to be given by:

$$F_{RS} = 1.9 \exp(-x'^{0.53}/1.2) \tag{3.9}$$

Another expression for the axial half-angle is:

$$\psi_{1/2} = 7.57\sqrt{\frac{a\psi_1}{d}} \quad \text{for} \quad \psi_1(rad) > \frac{a}{d} \ , \tag{3.10}$$

3.1.2 Axial $\chi_{\min}$ minimum yield/dechanneling probability

In this report we are equating the $\chi_{\min}$ minimum yield equations found in [5], which are usually associated with Rutherford Backscattering channeling spectra, with the probability that ions perfectly aligned to axial directions do not actually channel. This is because they are aimed into the open space between rows of atoms, but instead directly toward the top atoms of this row.

Two equations are given in [5] for the axial $\chi_{\min}$. The first is attributed to Lindhard [10] :

$$\chi_h^{<uvw>} = Nd\pi(2u_1^2 + a^2) \ , \tag{3.11}$$

and the second to Barrett [12] which is:

$$\chi_h^{<uvw>} = 18.8Ndu_1^2\sqrt{1+\frac{1}{\xi^2}} \ , \tag{3.12}$$

where

$$\xi = 126\frac{u_1}{(\psi_{1/2}d)} \tag{3.13}$$

We have selected the second form given by Barrett to use in the program.

3.1.3 Effect of amorphous overlayers on axial channeling

Not all crystals used as targets for channeling experiments are perfect all the way to the surface. Many have amorphous overlayers, e.g. the 15 *A* SiO_2 native oxide on the surface of Si. In addition, there is the use of Si implants into Si microelectronics to amorphize the near surface in order to avoid unwanted channeling that increases the junction depths of very shallow dopant implants. The effect of these overlayers was addressed and theoretically analyzed by Lugujjo and Mayer in their landmark paper in 1973 [13]. The equations and graph they derived for calculating the effect of these overlayers are included in Swanson's Appendix [5], and the graphical information is parameterized here.

According to Lugujjo and Mayer, the reduction of the $\psi_{1/2}$ half-angle due to small angle scattering due to the presence of amorphous overlayers is:

$$\theta_c = \frac{a_{13}E\psi_{1/2}}{(2Z_1Z_3e^2)} \ , \tag{3.14}$$

where Z_3 is the atomic number of the overlayer. We point out here that the equations in all three IBA handbooks [1,2,3] are wrong, because they do not agree with the Lugujjo and Mayer paper. This is because in all three Handbooks the Z_3 term in Equation 3.14 above, has been replaced by Z_2 and the value of *a* in equation 3.14 should be calculated for the Thomas-Fermi screening distance given for the incident ion in the overlayer, i.e.:

$$a_{13} = 0.04685 / (Z_1^{2/3} + Z_3^{2/3})^{1/2} \tag{3.15}$$

Now this is probably justified in the case of the native oxides or certainly Si amorphized layers on Si crystals, but the Lugujjo and Mayer paper derived expressions for the overlayer's effect on the channeling angle that was more generally applicable, i.e. for any overlayer of atomic number Z_3.

The increase in minimum yield, that we interpret as dechanneling probability $\chi_h^{<uvw>}$ is given by:

$$\chi_{\min} = P(\theta_c), \tag{3.16}$$

where the P function was given in graphical form in [13]. As in the previous cases where this information was graphical, we have parameterized $P(\theta_c)$, and in Figure 4 we show the results of that parameterization.

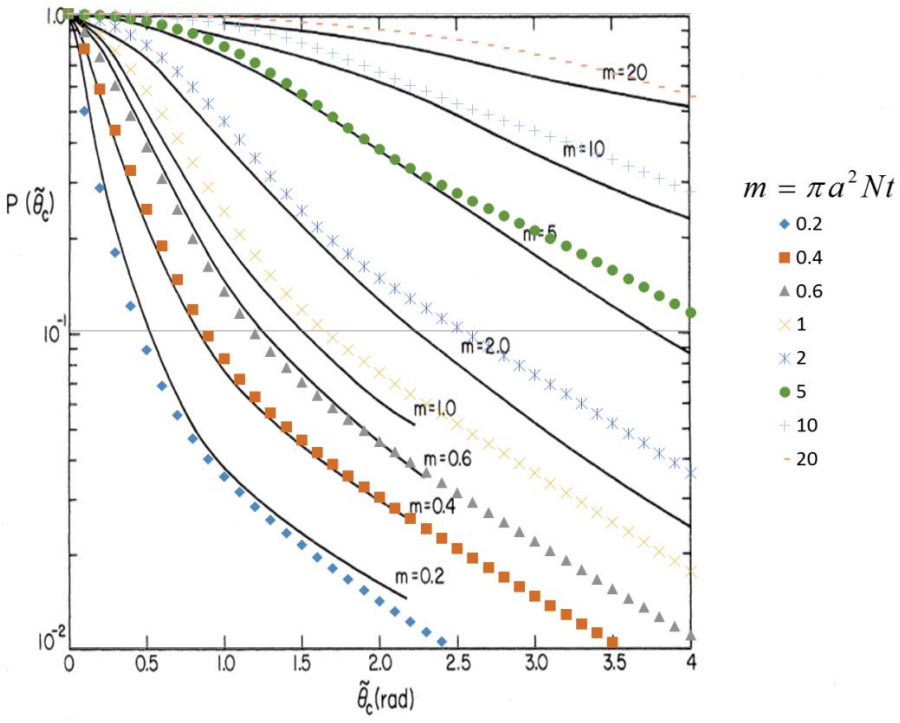

Figure 3 P function describing dechanneling due to amorphous overlayers together with the parameterization presented here.

In this parameterization the overlayer thickness parameter m is given by:

$$m = \pi a^2 Nt \tag{3.17}$$

Where a is the Thomas-Fermi screening distance given in Equation 3.15, N is the concentration of overlayer atoms per $Å^3$ and t is the thickness in *Å*. To check the accuracy of our parameterization of P, we compare to an example given in the Appendix of Ref. [13] for 1.8 MeV He^+ on <110> Si with two different overlayers.

	Overlayer	
1.8 MeV He->110 Si	**1550A Al**	**440A Au**
P(thc,m)= (this work)	0.22	0.61
P=(Ref. [13])	0.20	0.57

Table 1 Comparison of P(θ_c) from this parameterization and the example given in the Appendix of Ref. [13]

Again, just to be clear, the equations for the effect of overlayers on channeling half-angle and minimum yields should not be used as given in the IBA handbooks unless the surfaces are oxidized, or amorphized with self-ion implantation, but rather have overlayers of a different element.

3.2 Planar Channeling

3.2.1 Planar $\psi_{1/2}$ half-angles

The expression for planar $\psi_{1/2}$ half-angles is given in [5] as:

$$\psi_{1/2}^{p} = 0.72 F_{PS}\left(x', y'\right)\psi_a \ , \tag{3.18}$$

where

$$\psi_a = 0.545\sqrt{\frac{Z_1 Z_2 N d_p a}{E}} \ \ (degrees) \ . \tag{3.19}$$

N is the concentration of target atoms in units of #/$Å^3$ and d_p is the atomic separation of the planes (*Å*) for the usual [hkl] Miller index orientations, and Table A15.1 in [5] gives multiplicative factors for the lattice constants to get these separations, again for bcc, fcc and diamond lattices, but only up to [111].

The calculation of the separation of crystalline planes d_P from the standpoint of ion channeling is quite different from that for x-ray diffraction. This is because the coordinate system for diffraction is in reciprocal space, while that for channeling is in real space.

For bcc lattices, this factor is:

$$f_p^{bcc} = \frac{1}{\sqrt{h^2+k^2+l^2}} \text{ for } h+k+l = even \ , \tag{3.20}$$

or

$$f_p^{bcc} = \frac{1}{2\sqrt{h^2+k^2+l^2}} \text{ for } h+k+l = odd \ . \tag{3.21}$$

For fcc lattices, this factor becomes:

$$f_p^{fcc} = \frac{1}{\sqrt{h^2+k^2+l^2}} \text{ for } h,k,l \text{ all odd} \ , \tag{3.22}$$

or

$$f_p^{fcc} = \frac{1}{2\sqrt{h^2+k^2+l^2}} \text{ for } h,k,l = \text{ not all odd} \ . \tag{3.23}$$

For diamond lattices, the factor is:

$$f_p^{fcc} = \frac{1}{2\sqrt{h^2+k^2+l^2}} \text{ for all } h,k,l \text{ except permutations of [001]} \tag{3.24}$$

or

$$f_p^{fcc} = \frac{1}{4} \text{ for all permutations of [001] e.g. [010], [00}\bar{1}\text{] etc.} \tag{3.25}$$

d_p is then determined by multiplying the associate [hkl] factor by the conventional cell lattice constant.

$F_{PS}(x',y')$ in equation 3.12 is the square root of the adimensional planar potential using Moliere's screening function and also calculated using Monte Carlo techniques by Barrett [12]. The arguments in F_{PS} are:

$$x' = 1.6\left(\frac{u_1}{a}\right) \text{, and} \tag{3.26}$$

$$y' = \frac{d_p}{a} \tag{3.27}$$

The parameterized fit to the F_{PS} function plotted in A15.3 in [5] is shown in Fig. 3.

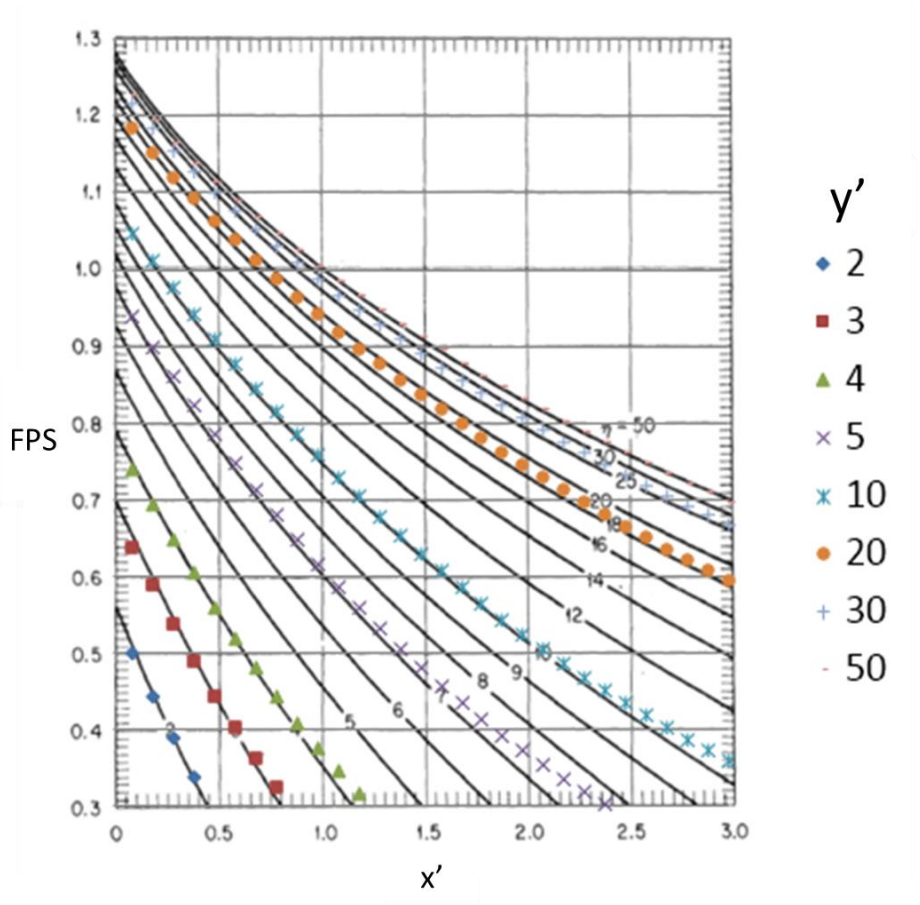

igure 4 Parameterization of the F_{PS} adimentional function for planar channeling

The equations used in this parameterization of the F_{PS} function are:

$$F_{PS} = F_{PSo}\exp(-x'^{p}/a) \tag{3.28}$$

$$F_{PSo} = 1.27(1-exp(-y'^{0.76}/3.0) \tag{3.29}$$

$$a = 4.3(1-exp(-y'^{1.1}/12) \tag{3.30}$$

$$p = 0.4exp\left(-y'/12\right)+0.85 \tag{3.31}$$

$\psi_{1/2}^{p}$ can then be calculated from Equation 3.18.

3.2.2 Planar $\chi_{\min}$ minimum yield/dechanneling probability

The equation given in [5] for the planar $\chi_{\min}$ was derived by Lindhard [10] and is:

$$\chi_h^{[hkl]} = \frac{2a}{d_p^{[hkl]}} \ . \tag{3.32}$$

4. COMPARISON WITH EXPERIMENTAL HALF-ANGLES GIVEN IN THE HANDBOOKS

The wonderful thing about the IBA Handbooks is that they not only contain all the equations for calculating channeling half-angles and minimum yields, but they also have a considerable amount of data generated by many of the researchers in the field of the $\psi_{1/2}$ values they measured. These measurements have been compared to the parametric calculations described above.

For planar half-angles the axial channeling data presented in [5] in Table A15.5, we compare the calculation of our parameterized half-angles and present that in Figure 5 below.

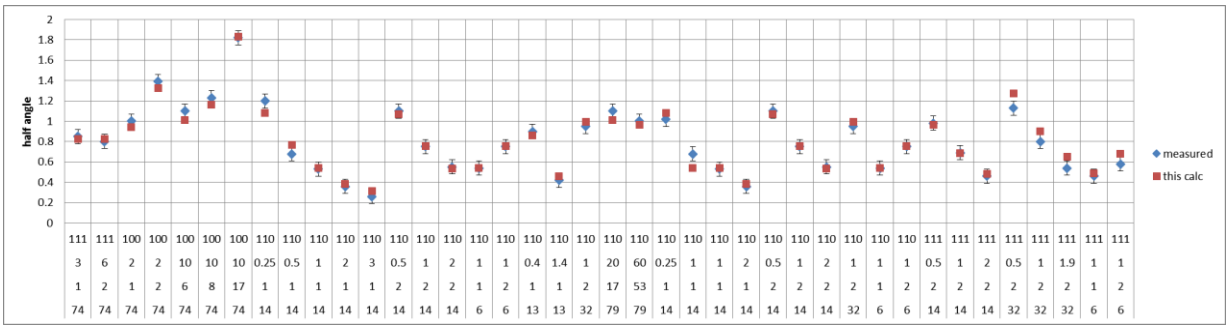

Figure 5 Measured half-angles in the IBA Handbooks of axial channeling compared to the calculations using the parameterizations developed here

In Figure 5, the numbers along the abscissa correspond from top to bottom to the <uvw> of the axis, the energy (MeV) and atomic number of the ion, and the atomic number of the target atoms. It should be pointed out that in order to get the best fit to the data plotted above, the prefactor was adjusted to be 0.87 so that the reduced χ_α^2 was 0.74 and the recommended equation for the axial channeling half-angle given here is:

$$\psi_{1/2}^a = 0.87 F_{RS}\left(x'\right)\psi_1 \tag{4.1}$$

For planar channeling the same analysis was done with all the data presented in Reference [5], and the prefactor of planar channeling adjusted to obtain the best fit. This resulted in the following figure and analysis:

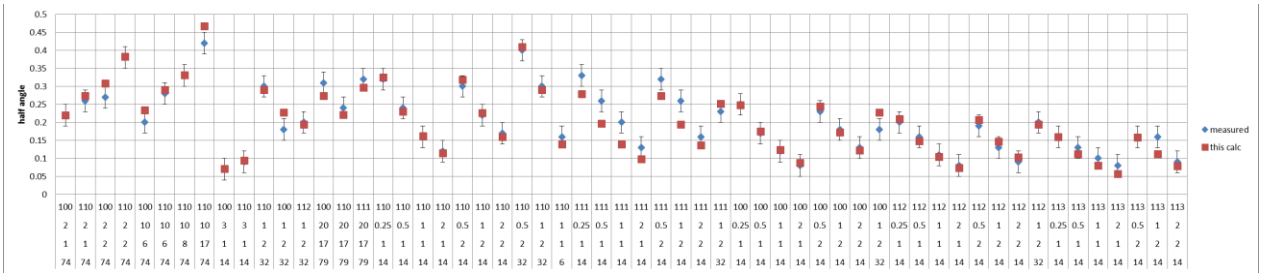

Figure 6 Measured half-angles in the IBA Handbooks for planar channeling compared to the calculations using the parameterizations developed here.

In Figure 6, the numbers along the abscissa correspond from top to bottom to the [hkl} of the plane, the energy (MeV) and atomic number of the ion, and the atomic number of the target atoms. As with the axial channeling calculations and their comparisons with the data presented in [5], the prefactor was adjusted to get the best fit, and this resulted in the best equation to use for calculating the planar channeling half-angle to be:

$$\psi_{1/2}^{p} = 0.65 F_{PS}\left(x', y'\right)\psi_a \qquad (4.2)$$

The prefactors used in Equations 4.1 and 4.2 are those used in the program.

5. STEREOGRAPHIC PROJECTIONS AND UNINTENTIONAL CHANNELING PROBABILITIES

As mentioned above, stereographic projections of the axial and planar channeling are normally used as a graphical way of navigating goniometers to axes and planes. We propose here that this type of visualization can also be used to assess the magnitude of accidental channeling. With the computationally automated calculation of $\psi_{1/2}$ half angles and $\chi_{\min}$ dechanneling factors, these projections can now be quickly determined for any <uvw> axis or [hlk] plane. This makes possible the generation and plotting of these projections with Excel. Filled black circles represent the effective channeling along axes, where their radius corresponds to the $\psi_{1/2}$ half angle times $(1-\chi_{\min})$ to provide a visualization of the degree of channeling down each axis. Grey-scaled lines are plotted for the planes where their width and darkness corresponds to the planar channeling ψ full width times $(1-\chi_{\min})$.

To avoid redundancy and an associated over-estimating of the accidental channeling probability, the program automatically rejects higher index <uvw> and [hkl] planes that have the same direction as lower index vectors. For example, the program rejects plotting and calculation of the accidental channeling probability for a <222> axis because it is identical to the <111> axis. There are 176 unique axes and planes for the case where the maximum indices are (555).

5.1 Equations for plotting stereographic projections

Stereographic projections are not simply projections onto a plane, say the xy plane in an orthogonal xyz coordinate system, of where <uvw> vectors intersect the unit sphere drawn around (0,0,0), nor the projection of 3D circles formed by the intersection of planes having [hkl] normal vectors on to the xy plane. But they are similar to this type of projection. If we define a point on the unit sphere of (x,y,z), there is a corresponding (θ,φ) or polar and azimuthal angles in the spherical coordinate system. In a stereographic projection this point has the same azimuthal angle φ, but the position of this point along the line defined by φ is linearly proportional to θ.

Because we are only considering cubic lattices, only the quadrant including the positive <uvw> axial channels need to be considered due to symmetry. They are the quadrants we plot in the remainder of this section.

5.1.1 Projection of axes

For an arbitrary <uvw> axis, we define the following parameters:

$$x = \frac{u}{\sqrt{u^2 + v^2}} \tag{5.1}$$

$$y = \frac{v}{\sqrt{u^2 + v^2}} \tag{5.2}$$

$$z = \frac{w}{\sqrt{u^2 + v^2 + w^2}} \tag{5.3}$$

The values for x and y provide the azimuthal φ in the projection:

$$\varphi = \tan^{-1}(y / x) \ , \tag{5.4}$$

And the z value gives the polar angle θ:

$$\theta = \cos^{-1}(z) \tag{5.5}$$

The position on the stereograph of an axial direction is then calculated using the following equations:

$$x' = x\theta \tag{5.6}$$

$$y' = y\theta \ , \tag{5.7}$$

and as indicated above, all of these <uvw> axes are plotted up to <555> axes as closed circles whose radii is scaled into the projection to be that of the effective $\psi_{1/2}$ half angle.

5.1.2 Projection of planes

To project planes, we first have to determine the equations for circles from the plane's intersection with the unit sphere, and then use the equations above. While this involves a considerable amount of geometry and algebra, it reduces to generating in parametric form the 3D coordinates of a circle on the unit sphere that has a normal vector given by [hkl]. This equation is:

$$\vec{P}(t) = \cos(t)\vec{u} + \sin(t)(\vec{n} \text{ x } \vec{u}) \ , \tag{5.8}$$

where equations 5.4 and 5.5 give the values for θ and φ using i for u, j for v, k for w. in Equations 5.1-3 above.

$$\vec{u} = \begin{pmatrix} -\sin(\varphi) \\ \cos(\varphi) \\ 0 \end{pmatrix}, \text{ and} \tag{5.9}$$

$$\vec{n} \text{ x } \vec{u} = \begin{pmatrix} \cos(\theta)\cos(\varphi) \\ \cos(\theta)\sin(\varphi) \\ -\sin(\theta) \end{pmatrix}, \tag{5.10}$$

Taking the vector sum in Equation 5.8, the values for x and y are obtained from:

$$\begin{pmatrix} x(t) \\ y(t) \\ z(t) \end{pmatrix} = \vec{P}(t) \tag{5.11}$$

Equations 5.6 and 5.7 then take these x and y values into the (x'(t),y'(t)) stereographic coordinate system. The program then calculates a set of (x',y') coordinates for each [hkl] plane and their +/- permutations (i.e. $[111],[\bar{1}11],[1\,\bar{1}1]$ etc) by stepping t from 0 to 360° and plotting these points as lines in Excel where the line width is scaled to correspond to the full effective ψ^p planar channeling angle (i.e. $\psi^p(1-\chi_{\min})$) calculated using Equation 3.18. To increase the visualization of planar channeling magnitude, the lines are also plotted in gray-scale where their darkness corresponds to the effective planar channeling ψ^p full width.

5.2 Examples of stereographic projections

One must take care in over interpreting the results calculated by the program for the extremely high order axial and planar channeling calculations of $\psi_{1/2}$ of axes or planes. For this reason we limit ourselves here to calculations of $\psi_{1/2}$ for axes and planes to (555). While the program includes all these axes and planes, the calculation of accidental channeling and presentation of stereograms, can be limited to whatever the user of the program desires, e.g. (222).

5.2.1 Rutherford Backscattering (RBS) Channeling

5.2.1.1 High Energy

Stereographic projections useful for MeV-energy RBS channeling are show here. The stereographs have been calculated for 1 MeV C ions to accentuate the half-angles. The target crystal was selected to be Fe, Cu and Ge to illustrate how these stereographs differ for similar atomic number targets that have bcc, fcc and diamond crystal symmetry. These projections are plotted for Cu, Fe and Ge in Figures 7,8, and 9 respectively below. The graphs are plotted without the usual θ curves to avoid cluttering these plots.

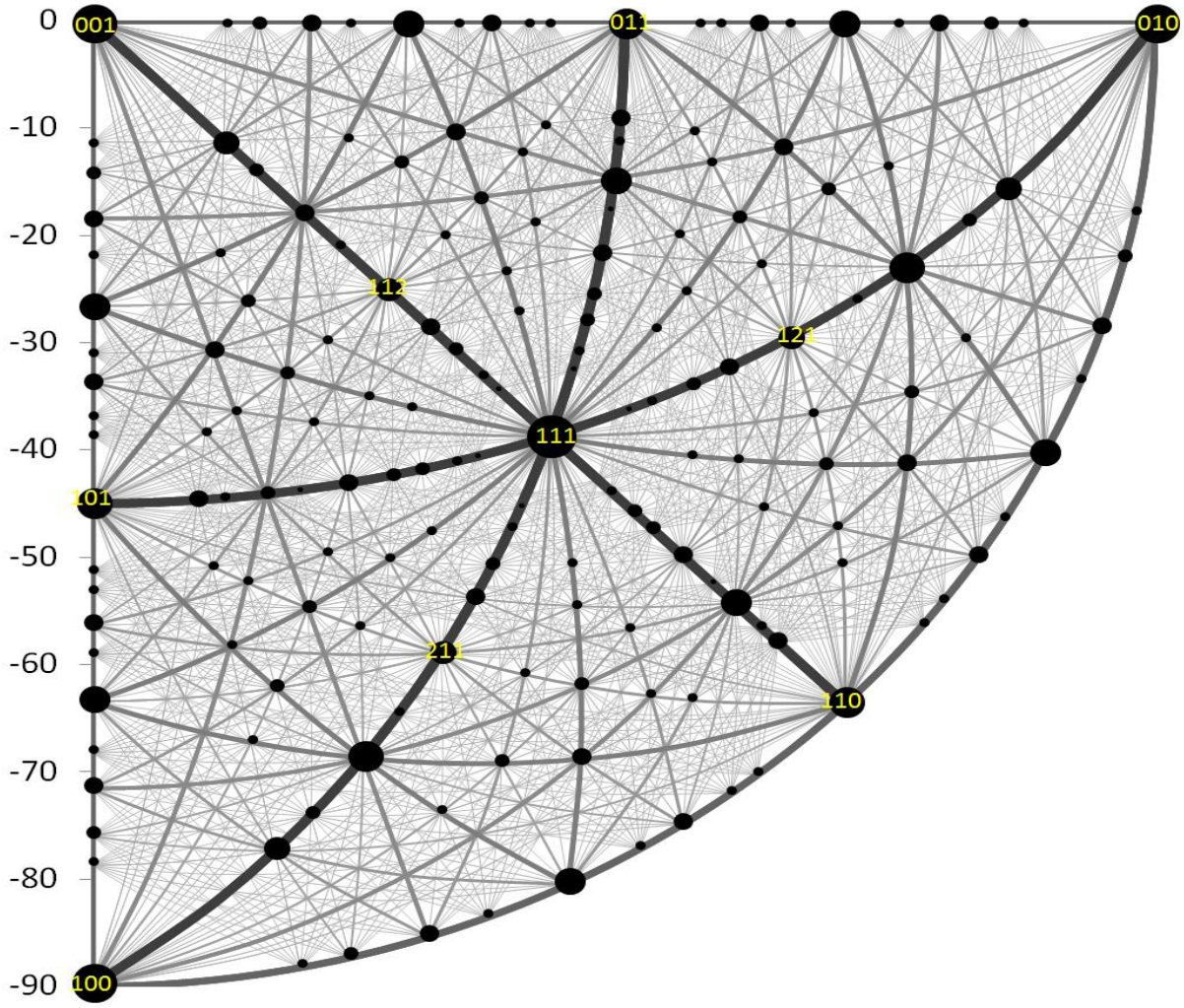

Figure 7 Stereographic projection of axial and planar channeling of 1 MeV C in bcc Fe

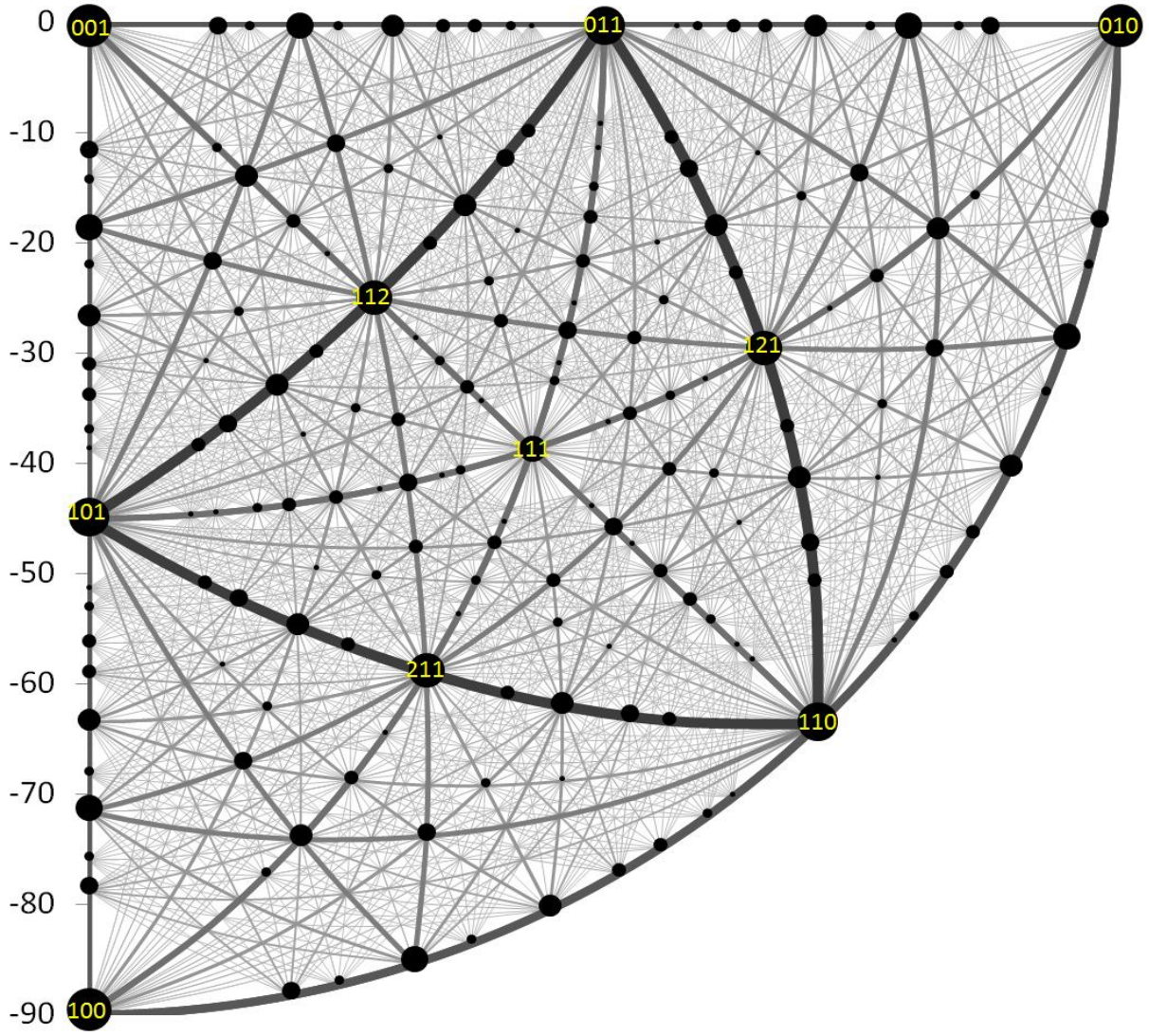

Figure 8 Stereographic projections of axial and planar channeling of 1 MeV C in fcc Cu

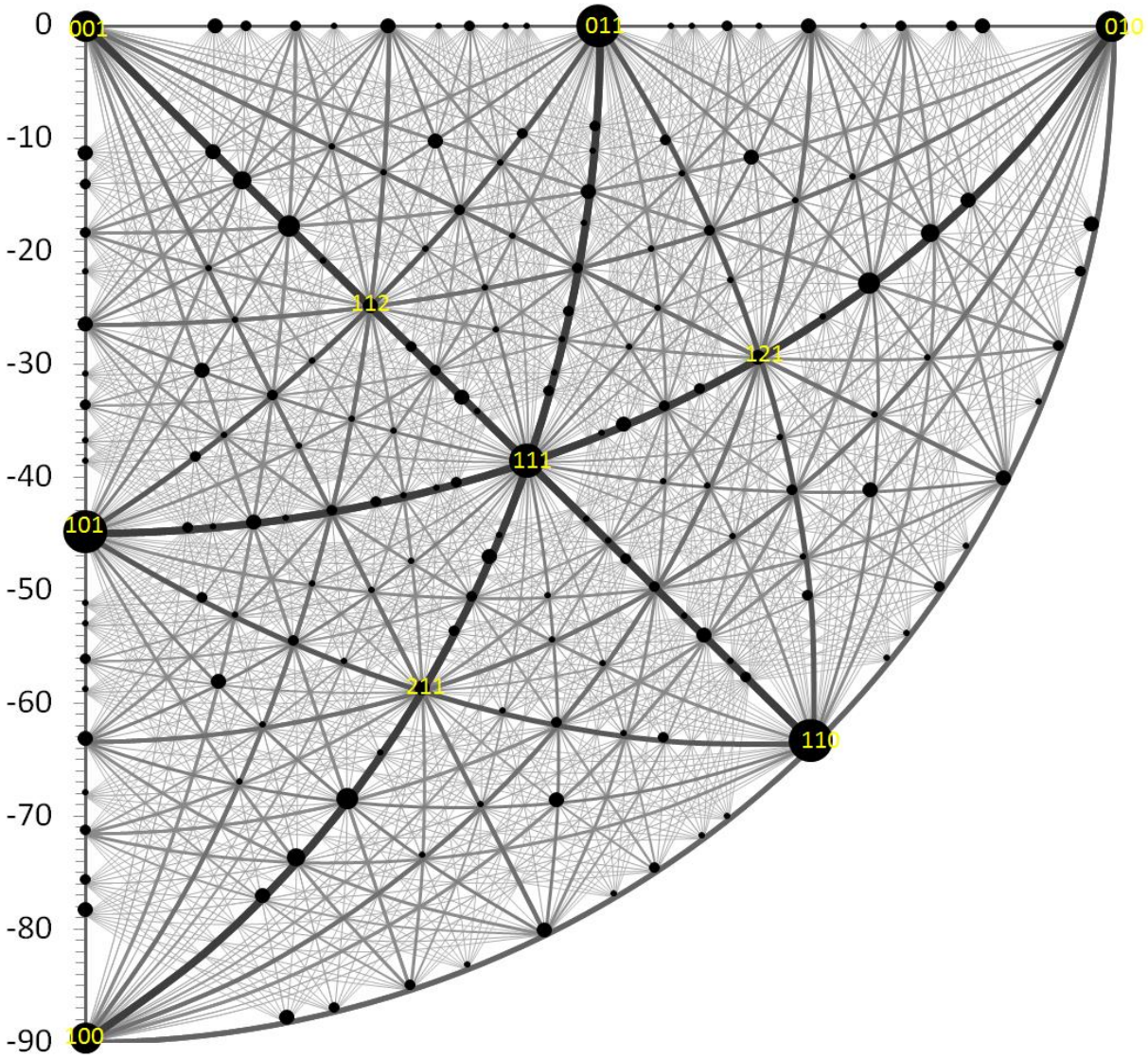

Figure 9 Stereographic projections of axial and planar channeling of 1 MeV C on diamond Ge

5.2.1.2 Low Energy

As mentioned above, ion channeling is starting to be performed using He ion Microscopes (HIM) [7]. The He energy is generally between 15 and 30 keV. The stereogram in Figure 9 was calculated for 15 keV He on fcc Au which can be compared to the stereographic projection presented for the same conditions in [7].

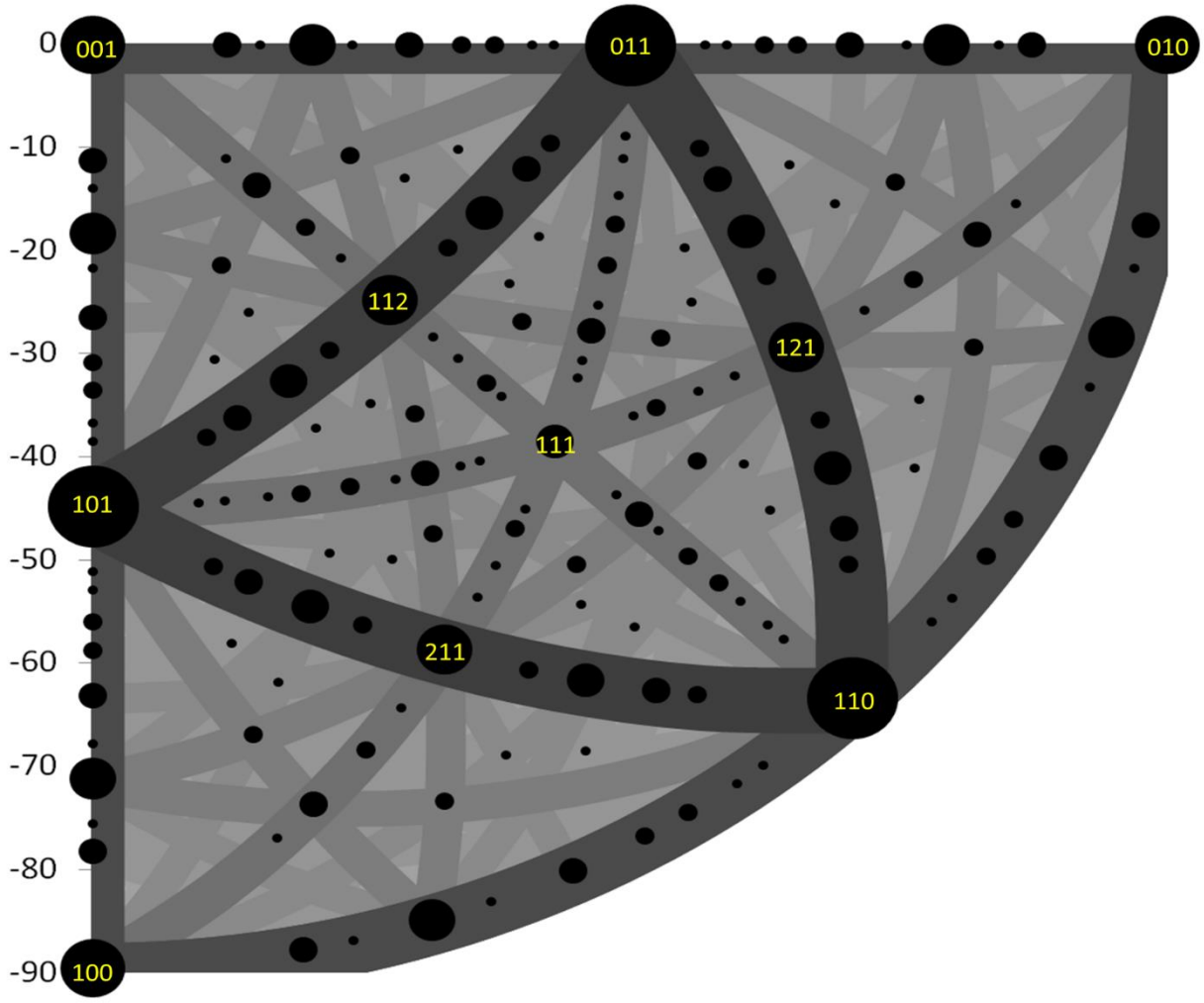

Figure 10 Stereographic projection of axial and planar channeling of 15 keV He in fcc Au

A qualitative agreement is found when comparing this projection to that found in [7], particularly the small axial channeling predicted for <111> compared to the permutations of <011>.

5.2 Accidental Channeling

In this section we address the calculation of accidental or unintentional channeling probabilities. As indicated above this has been predicted to be of consequence in [8] as regards the different

degree to which crystalline nanograins in metals can be damaged by high energy heavy ions. These ion exposures are used to simulate the displacement damage produced in nuclear reactor materials by the high fluences of energetic neutrons during their lifetime. If these nanograins are oriented so that the ions channel, they will experience less displacement damage and swell less than those grains not so oriented. This could obviously affect mechanical properties.

The ions used in [8] were 2 MeV ions of Si, Cu and W exposed to a nanocrystalline solid of bcc W. The stereographic projections for up to (555) orientations of axes and planes is shown for all three of these ions in Figure 10.

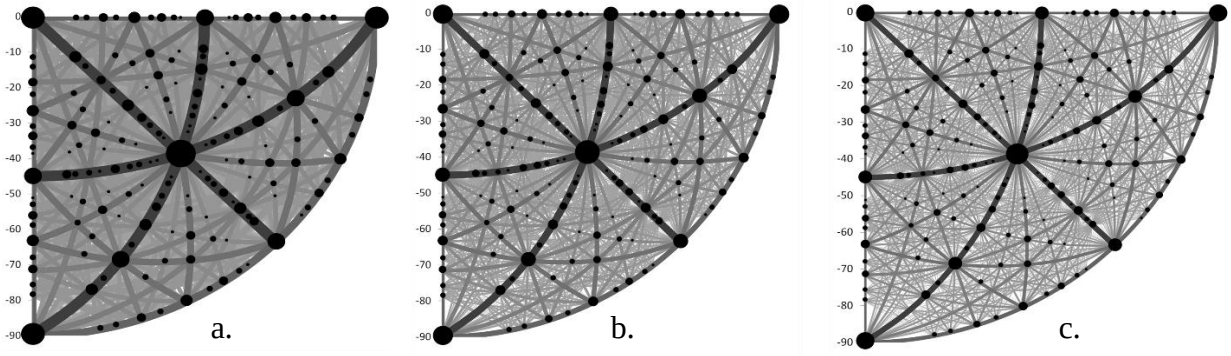

Figure 11 Stereographic projections from left to right a,b,c of 2 MeV W, Cu and Si respectively on bcc W.

These projections show that the channeling half-angles clearly depend on the atomic number of the projectile. They also dramatically show the hazard of overintepreting accidental channeling probabilities if the highest order axes and planes are used. This is because of the overlap of the planes, which is not included in the program. For this reason, we restrict the calculation of channeling probabilities to orders of (222).

These probabilities are calculated as follows. For axial channeling, the axes on the corners of the stereograms are considered to contribute an angular area of $1/4\,\pi\psi_{1/2}^2$ in radians to the total axial channeling in this quadrant, these are the <001>, <010> and <100> axes. The axes on the edges of the quadrant contribute $1/2\,\pi\psi_{1/2}^2$ and the axes in the central region a full $\pi\psi_{1/2}^2$. Now we are calling this a quadrant because of how its projected, but there are really 8 of these quadrants, and so to get the total angular area, the sum of all of the axes areas in this quadrant is multiplied by 8. To get the axial channeling probability we then just divide this sum of angular areas by 4π.

For planar channeling we first calculate $2\pi\psi^p$ for the planar full angles each unique [hkl] planes up to [222] (there are 20 for the indices all positive). The sum of all these planar angular areas is then divided by 4π to get the planar channeling probability.

Table 2 shows the results of these calculations for the exposures in [8] and for the stereograms above.

	channeling probability		
2 MeV	axes	planes	total
W->W	0.037	0.326	0.363
Cu->W	0.027	0.219	0.246
Si->W	0.020	0.157	0.178

Table 2 Channeling probability for 2 MeV W, Cu and Si on W.

For the exposure conditions used by El-Atwani [8] to simulate neutron damage in W nanocrystals, there was a considerable amount of channeling occurring. How this relates to the accidental channeling that occurs with neutron exposures is unknown, and this needs to be a subject for further research.

On the one hand if one considers hard sphere recoiling by fission neutrons that have an average energy of 3 MeV, the average recoil of W will have only 33 keV. Using indices only up to (111), the axial accidental channeling then goes up to 18% and for the planes it actually goes above 1! This isn't physically possible for the planes, and is a shortcoming of the program by not considering overlaps.

On the other hand, all of the W recoils must originate from a lattice site, and that could significantly reduce the chance that it takes a trajectory that channels. Better calculations need to be made involving the use of nuclear recoiling cross sections, and molecular dynamics.

In either case, however, it is clear that channeling could reduce the damage of poly-crystalline metals exposed to the neutrons produced in nuclear reactors. Calculations that do not include the effect of channeling may significantly overestimate the amount of displacement damage. Channeling may therefore extend the useful life of structural reactor components and claddings of reactor fuel.

6. CONCLUSIONS

This report gives all the equations and parameterization of graphical representations of Monte-Carlo calculations of ion channeling to determine the half-angles for axial and planar channeling and with these angles determine the accidental or unintended channeling of implanted ions, or those recoiled by neutrons an primary knock on atoms in polycrystalline metals in nuclear fission or future fusion reactors.

The program uses all the equations both derived from basic physics by Lindhard [10] and those parameterized here from Barrett's Monte-Carlo calculations [12] . This program has been developed in universally available MS Excel together with macros in Visual Basic Applications (VBA).

The program can calculate the axial and planar half-angles for channeling given only the atomic number and energy of the projectile, and the atomic number of the target. The indices of these axes and planes can go up to (555), as this seem a practical limit to the use of the channeling equations and parameterized graphs.

This information can be used for individual <uvw> axis or [hkl] planes, or with the program to generate these half angles for all axes and planes up to (555). This information can be used in turn to generate stereographic projections of the axial and planar channeling by virtually any ion in any crystalline or polycrystalline target. All of the equations for ion channeling and the generation of these stereographic projections are given in this report.

The impetus for these calculations was a paper written in collaboration with Sandia by El-Atwani et. al [8] where the effects of ion channeling on the reduction of MeV-energy heavy ions on nanocrystalline samples of W studied with Sandia's unique in-situ ion irradiation TEM, The I^3TEM was used to observe the accumulation of such damage in real time. The most substantive physics to be taken from this report is that the effects of ion channeling may dramatically reduce the effects of displacement damage by the recoil of polycrystalline material atoms used just outside of the nuclear fuel, i.e. the claddings, and even in the structural materials used outside the reactor.

The ease of generating stereographic projections of both axial and planar channeling where the dimensions of the half-angles are represented in these plots, is of scientific value to the assessment of channeling effects. It would be remiss to not report that these projections are also beautiful, and show physics at its best, highly informational, instructional and spectacular to observe.

References

1) "Ion Beam Handbook for Material Analysis", Ed. J.W.Mayer and E. Rimini, Academic Press, Inc (1977).
2) "Handbook of Modern Ion Beam Materials Analysis", Ed. J.R. Tesmer and M. Nastasi, Materials Research Society ISBN 1-55899-254-5 (1995) .
3) "Handbook of Modern Ion Beam Materials Analysis – Second Edition", Main Volumn and Appendices, Ed. Y. Wang and M. Nastasi, Materials Research Society ISBN 978-1-60511-215-2 (2009).
4) Ibid 1, B.R. Appleton and G. Foti, Chapter 3 "Channeling" (1977) 67.
5) Ibid 2, M.L. Swanson, Chapter 10 "Channeling" (1995) 231and Appendix 15 "Channeling Data" (1995) 643.
6) Ibid 3, M.L. Swanson and L. Shao, Chapter 12 "Ion Channeling" (2009) 247 (in Main) and Appendix 17 "Ion Channeling Data" (2009) 309 (in Appendices).
7) V. Veligura, G. Hlawacek, R. van Gastel, H.J.W. Zandvliet and B. Poelsema, Beilstein Journal of Nanotechnology, Vol. 3 (2012) 501.
8) O. El-Atwani, A. Suslova, T.J. Novakowski, K. Hattar, S.S. Harilal and A. Hassanein, NEED SUBMISSION STATUS.
9) Ibid 8, reference 51.
10) Lindhard, J., *Mat.-Fys. Medd.: K. Dan. Vidensk. Selsk.*, **34** (1965), No. 14
11) Firsov, O.B., *Soviet Phys*. **JETP 6**, (1958), p. 534
12) Barrett, J.H., *Phys. Ref*. **B3**, (1971) p. 1527
13) E. Lugujjo and J.W. Mayer, Phys. Rev B7 (1973) 1782.

DISTRIBUTION

1	MS1056	Jon Custer	01111
1ea	MS1056	All Dept. Staff	01111
1	MS0899	Technical Library	9536 (electronic copy)


Sandia National Laboratories